

Color-Tuning Strategy for Iridapolycycles $[(N^{\wedge}N)Ir(C^{\wedge}C)ClPPh_3]^+$ by the Synergistic Modifications on Both the $C^{\wedge}C$ and $N^{\wedge}N$ Units

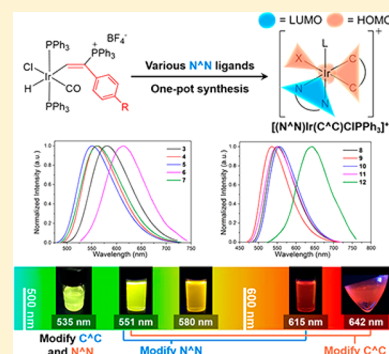
Zi-Ao Huang,[†] Qing Lan,[†] Yuhui Hua,[†] Zhixin Chen,[†] Hong Zhang,^{*,†} Zhenyang Lin,[‡] and Haiping Xia[†]

[†]State Key Laboratory of Physical Chemistry of Solid Surfaces and Collaborative Innovation Center of Chemistry for Energy Materials (iChEM), College of Chemistry and Chemical Engineering, Xiamen University, Xiamen 361005, China

[‡]Department of Chemistry, The Hong Kong University of Science and Technology, Clear Water Bay, Kowloon 999077, Hong Kong

S Supporting Information

ABSTRACT: The luminescent studies of cyclometalated Ir(III) complexes have attracted considerable interests in recent years. To fulfill the needs of emission wavelengths in various areas, the strategic emission color tuning of iridium(III) complexes is vital for their applications as phosphorescent materials. However, a feasible color-tuning method for iridacycles with fused carbon-rings ($C^{\wedge}C$) has not been reported yet. Herein, a convenient color-tuning strategy for $C^{\wedge}C$ -based Iridacycles is accomplished with the aid of DFT calculations. The developed synthetic protocol allowed facile modifications on $C^{\wedge}C$ units and $N^{\wedge}N$ units via a one-pot synthesis starting from iridium vinyl complexes, accessing the novel phosphorescent iridapolycycles $[(N^{\wedge}N)Ir(C^{\wedge}C)ClPPh_3]^+$.



INTRODUCTION

Cyclometalated Ir(III) complexes have been widely employed in organic light-emitting diodes (OLEDs),¹ chemosensors,² bioimaging,³ photocatalysts,⁴ and other fields⁵ over the past few years. Their excellent luminescent properties include high quantum yield at room temperature and relatively long phosphorescent lifetime. In addition, the tunable emission color is also considered as an advantageous feature⁶ due to varied needs of emission wavelengths from different application areas.

A variety of cyclometalating ligands ($C^{\wedge}N$ ligand) and ancillary ligands ($N^{\wedge}N$ or $L^{\wedge}X$ ligand) have been exploited to form Ir(III) complexes with specific characteristic emission wavelength.⁷ Density functional theory (DFT) calculations have recently been used to study these unique complexes with the aim of obtaining a quantitative structure–property relationship elucidation.⁸ For example, the highest occupied molecular orbital (HOMO) of a 2-phenylpyridyl Ir(III) complex mainly localized on metal center and the phenyl rings, whereas the lowest unoccupied molecular orbital (LUMO) primarily distributed on the pyridine rings.⁹ Therefore, structural modifications targeted at increasing/decreasing of the energy gap between HOMO and LUMO could achieve the blue-/redshift of the emission peaks. So far, most of these approaches involve strategic emission wavelength tuning of $C^{\wedge}N$ -based cyclometalated Ir(III) complexes.¹⁰ Surprisingly, there are no reports on rational color-tuning strategy for iridacycles with metal core embedded in the all-carbon rings ($C^{\wedge}C$) to the best of our knowledge. Only very few studies have been reported on the luminescent properties of iridacycles

with metal-embedded cyclic all-carbon frameworks,¹¹ although the related synthesis and reactivity of these iridacycles have been widely investigated,¹² thus posing limitations in the development of color-tuning strategy.

We have previously demonstrated that iridacyclopentadiene derivatives represent a promising scaffold for intriguing modification of emission wavelength.¹³ However, the quantum yields of these iridacyclopentadiene derivatives are not sufficient to be used as phosphorescent materials, partially due to the inappropriate orbital distribution in the LUMO. In addition, multistep synthesis and time-consuming purification were required for the previous synthetic manipulations to obtain these phosphorescent iridapolycycles. Hence, a convenient method to obtain iridapolycycles would circumvent the need for tedious structural modification, thereby providing an efficient color-tuning strategy for $C^{\wedge}C$ -based iridacycles.

Herein we developed a sequential color-tuning strategy that is efficient for iridapolycycles $[(N^{\wedge}N)Ir(C^{\wedge}C)ClPPh_3]^+$ to simultaneously achieve enhancement of the emission intensity and multicolor emission (Figure 1). DFT calculations disclosed the orbital distributions in the HOMO/LUMO of these $C^{\wedge}C$ -based complexes, which indicated modifying the $N^{\wedge}N$ ligand and $C^{\wedge}C$ ring should result in fine color tuning of efficient phosphorescence emission in the visible region. On the basis of computational studies, further structural modification leading to a particular color shift and satisfactory phosphorescent efficiency has been achieved.

Received: September 13, 2017

Published: December 7, 2017

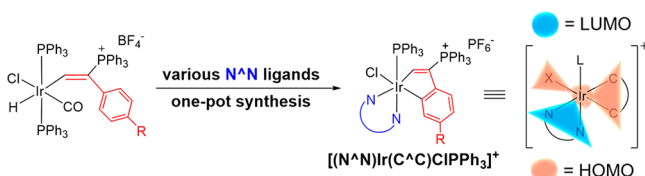


Figure 1. Sequential color-tuning strategy for iridapolycycles $[(N^N)Ir(C^C)ClPPh_3]^+$ via a one-pot synthesis from iridium vinyl complexes.

RESULTS AND DISCUSSION

Structural Design with the Aid of Computational Analysis. Our previous work shows that iridapolycycle **3** can be obtained through the reaction of benzo-iridacyclopentadiene (**2-benzo**) with 2,2-bipyridyl (**Scheme 1**).¹³ The HOMO of **3** is

Scheme 1. Synthesis of Compound **3** via the Reaction of **2-benzo** with 2,2-Bipyridyl



mainly localized on metal center and the C^C framework, which almost does not overlap with its LUMO (**Figure 2**).

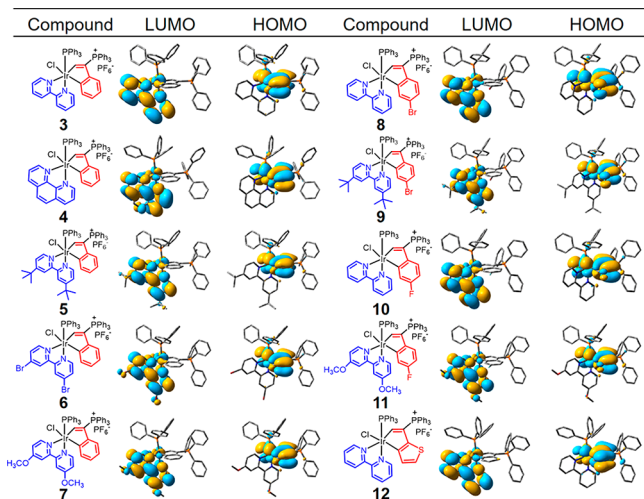


Figure 2. Chemical structures and orbital distributions in LUMO/HOMO of iridapolycycles **3–12**. DFT calculations were performed using the Gaussian 09 suite of programs,¹⁴ and the LANL2DZ basis set¹⁵ was used to treat the Ir, P, Br, S, and Cl atoms, whereas the 6-31G basis set was used to treat all other atoms.

Thus, we speculated that unique orbital distribution in the HOMO/LUMO of **3** can be exploited to achieve emission color tuning by modifying the C^C units and N^N units, respectively.

To test this possibility, a series of iridapolycycles (**4–12**, **Figure 2**) with different C^C or N^N structures used as templates were surveyed computationally to investigate the effect of structural modulation on the photophysical properties. DFT calculations were performed on these iridapolycycles to estimate the orbital distributions in their HOMO/LUMO (**Figure 2**) and energy levels (**Figure 3**). As expected, all these

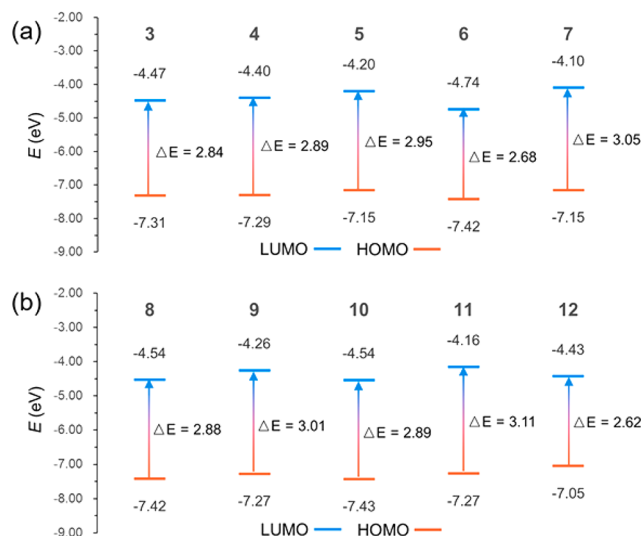


Figure 3. Calculated HOMO and LUMO levels of iridapolycycles (a) **3–7** and (b) **8–12**.

iridapolycycles display similar orbital distributions in their HOMO/LUMO to those of **3**, indicating the possibility for color-tuning approaches based on tailoring the C^C units and N^N units of these iridapolycycles.

As shown in **Figure 3**, modification of N^N ligands leads to strong influence in the energy gaps (ΔE s) of compounds **4–7**. The changes in ΔE are dominated by the differences of their LUMOs. For example, compound **4** with a more rigid N^N ligand (1,10-phenanthroline) has increased energy levels of both LUMO and HOMO compared to **3**, yet the ΔE of **4** is increased due to a higher energy LUMO. Similar trends can be found in other iridapolycycles. For **5** and **7**, electron-donating *tert*-butyl and methoxyl groups on the N^N unit give rise to the increase of their LUMO energy levels, leading to greater ΔE s when compared with **3**, whereas the electron-withdrawing bromine atoms on the N^N ligand of **6** result in a significant decrease in its LUMO energy level and ΔE . Therefore, altering the N^N ligands has a much greater impact on the energy levels of LUMO, which could be employed as a tuning strategy toward their LUMO energy levels.

As for the C^C modifications of iridapolycycles, the HOMO energy levels can be dramatically affected, resulting in considerable differences in the ΔE s calculated for **3**, **8**, **10**, and **12**. For example, electron-withdrawing halogen atoms on the C^C units of **8** and **10** lead to lower HOMO energy levels and increased ΔE s, while the replacement of the benzene ring in the C^C unit with an electron-rich thiofuran ring can increase the HOMO energy level and obviously reduce ΔE of iridapolycycle **12**. Thus, a tuning method toward the HOMO energy levels of iridapolycycles could be achieved by C^C modifications based on the DFT calculations.

The effect of simultaneous modifications of the C^C and N^N units was also investigated by model iridapolycycles **9** and **11**. In comparison with **5** and **8**, the ΔE of **9** is even larger due to the cooperative effect of an electron-donating group on the N^N unit and an electron-withdrawing group on the C^C unit. Similarly, the larger ΔE of **11**, compared with **3**, **7**, and **10**, also demonstrates the feasibility of the combined tuning strategy via modifications on C^C and N^N sequentially.

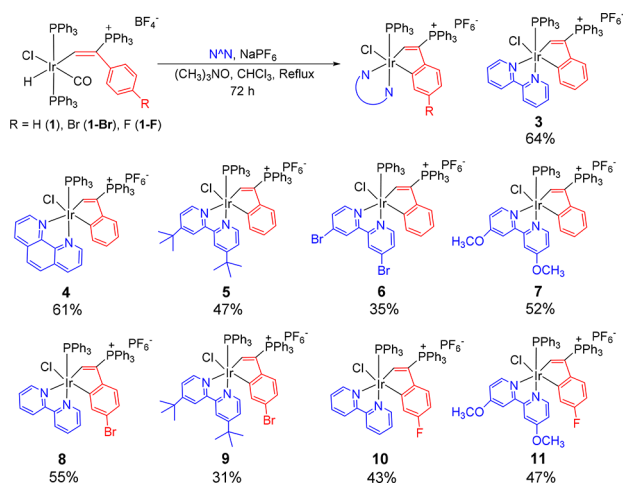
To further estimate the consistency of calculation results and experimental findings, the lowest singlet (S_1) and triplet states

(T_1) of compounds 3–12 were investigated by TD-DFT calculations (Table S2). According to the computational results, all the lowest excited states S_1 and T_1 of those compounds can be attributed to the transition from HOMO to LUMO without exception. On the basis of the frontier orbital distribution, a combination of $[d\pi(\text{Ir}) \rightarrow \pi^*(\text{N}^{\wedge}\text{N})]$ metal-to-ligand charge transfer (MLCT) and $[\pi(\text{C}^{\wedge}\text{C}) \rightarrow \pi^*(\text{N}^{\wedge}\text{N})]$ ligand-to-ligand charge transfer (LLCT) is responsible for the emission nature of 3–12. Thus, the ΔE s between HOMO and LUMO of 3–12 were expected to be consistent with their phosphorescent energies, leading to blue-shifted emissions found in 4, 5, and 7–11 with higher ΔE s and red-shifted emissions found in 6 and 12 with lower ΔE s, in comparison with those of 3.

DFT calculations were performed to estimate the influence of the grafting position of the substituents on the color-tuning direction of the compounds. According to the frontier molecular orbitals for compounds 13'–15' (Table S3), the position change of *tert*-butyl group from the para site to para site of the $\text{N}^{\wedge}\text{N}$ ligand leads to a significant increasing of the ΔE s of 13'; however, the shift of bromine position on $\text{N}^{\wedge}\text{N}$ ligand rarely changes the ΔE s. Besides, the effect of substituents position on $\text{C}^{\wedge}\text{C}$ ligand is not obvious, according to the comparison of ΔE s of compounds 15' and 8.

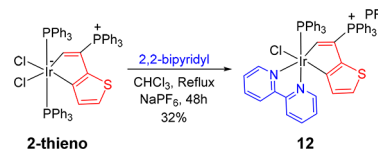
Synthesis and Characterization. On the basis of the above computational analysis, iridapolycycles 4–12 were synthesized to accomplish the color-tuning strategy experimentally. Unlike the traditional color-tuning methods for $\text{C}^{\wedge}\text{N}$ -based cyclometalated Ir(III), the easy-to-prepare iridium vinyl complexes have been introduced in this method as a main contribution for HOMO orbital. To simplify our previous reaction procedure, we tested a one-pot synthesis method to prepare the iridapolycycles directly from iridium vinyl complexes. To our delight, 4–12 were efficiently synthesized by treatment of 1, 1-Br, or 1-F with the corresponding $\text{N}^{\wedge}\text{N}$ ligands in the presence of trimethylamine oxide and sodium hexafluorophosphate under refluxing in chloroform (Scheme 2). In addition, a 64% yield of 3 was achieved by the one-pot synthesis, which is slightly higher than our previously reported method¹³ (60%, the yield of 2-benzo was considered). In this event, compound 12 is failed to be obtained through this one-pot method from the corresponding iridium vinyl complex. Compound 12 can only be synthesized by treatment of 2-

Scheme 2. One-Pot Synthesis for Iridapolycycles $[(\text{N}^{\wedge}\text{N})\text{Ir}(\text{C}^{\wedge}\text{C})\text{Cl}(\text{PPh}_3)]^+$ from Iridium Vinyl Complexes



thieno¹³ with 2,2-bipyridyl via a ligand substitution reaction (Scheme 3). All the iridapolycyclic products have been characterized by multinuclear NMR spectroscopy and elemental analysis.

Scheme 3. Synthesis of Iridapolycycles 12 from Thieno-iridacyclopentadiene 2-thieno



The structures of 4–6, 8–10, and 12 have also been confirmed by X-ray diffraction. The crystallographic details are listed in Table S1, and their selected bonds distances and angles are listed in Table 1. X-ray structural analysis (Figure 4) shows that these iridapolycycles adopt approximate octahedral geometry, having the $\text{N}^{\wedge}\text{N}$ units perpendicular to the coplanar $\text{C}^{\wedge}\text{C}$ frameworks. The Ir1–C1 (1.988(8)–2.022(5) Å) and Ir1–C4 (2.021(7)–2.042(7) Å) bonds are of similar lengths to what was found in 3 (1.981(7) Å and 2.027(7) Å). The bond distances and bond angles in these structures are nearly identical despite the different $\text{N}^{\wedge}\text{N}$ ligands and substituents bearing on the $\text{C}^{\wedge}\text{C}$ units.

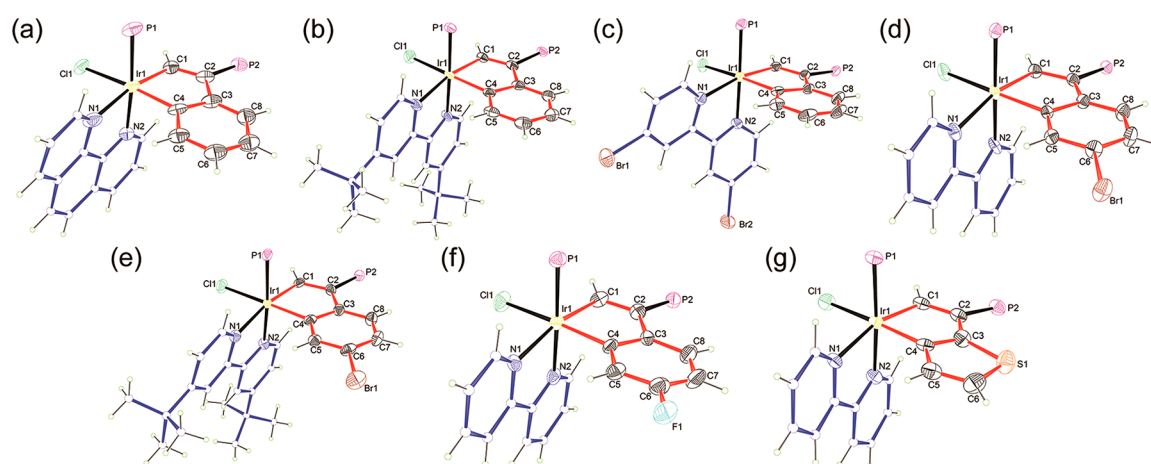
The thermal stability and photostability of these iridapolycycles were evaluated by taking 3–5 and 8 as representative examples (Table S4). As indicated by NMR spectrometry, all the solid samples remain unchanged at 160 °C in air for at least 10 h, with slight decomposition appeared after 14 h. In addition to the acceptable thermal stability, 3–5 and 8 show excellent photostability in deuterated CH_2Cl_2 under 7 days of irradiation by 12 W blue LEDs (12 W). No significant decomposition was observed on the fifth day and less than 5% of the compounds decomposed on the sixth day (Table S5). The solubilities of 3–5 and 8 were also tested. As shown in Table S6, 3–5 and 8 are highly soluble in dichloromethane (DCM), chloroform, tetrahydrofuran (THF), DMSO, and acetone, while they show very low solubility in toluene and H_2O . The solubility in toluene of these compounds can be increased significantly when a little amount DCM or chloroform is added, but they barely dissolve in a 1:1 DMSO– H_2O mixture.

Since triphenylphosphonium groups (PPh_3^+) have been generally introduced in molecular probes targeting mitochondria,¹⁶ these iridapolycycles bearing PPh_3^+ could be expected to achieve specific subcellular localization in bioimaging. Although lipophilicity can facilitate the shift through phospholipid bilayers of mitochondria,^{16b} the hydrophilic groups is often adopted to reduce the cytotoxicity of the systems.¹⁷ Thus, the balance of hydrophilicity and lipophilicity might also be important for iridapolycycles 4–12 to be exploited as biosensing probes.

Photoluminescence Properties. The emission maxima (λ_{em}), absolute PL quantum yield (Φ_{PL}), and luminescent lifetime (τ) of 4–12 are measured and summarized in Table 2. Red-emissive iridapolycycles 6 and 12 have significant reduced Φ_{PL} and τ . Meanwhile, the introduction of methoxyl groups to $\text{N}^{\wedge}\text{N}$ ligand of $[(\text{N}^{\wedge}\text{N})\text{Ir}(\text{C}^{\wedge}\text{C})\text{Cl}(\text{PPh}_3)]^+$ also evokes reductions of Φ_{PL} and τ in 7 and 11. On the basis of their Φ_{PL} and τ data, the experimentally measured radiative and nonradiative rate constants (k_r and k_{nr} , respectively) of 4–12 were summarized

Table 1. Selected Bond Distances (Å) and Bond Angles (deg) in 4–6, 8–10, and 12

	4	5	6	8	9	10	12
Ir1–C1	2.013(8)	1.997(4)	2.002(5)	1.990(4)	1.996(5)	1.988(8)	2.022(5)
Ir1–C4	2.025(8)	2.042(5)	2.036(5)	2.036(4)	2.035(5)	2.021(7)	2.023(5)
Ir1–P1	2.293(2)	2.2924(12)	2.2857(12)	2.2943(11)	2.2875(13)	2.289(2)	2.2882(12)
Ir1–Cl1	2.4975(19)	2.4858(13)	2.4862(12)	2.4938(10)	2.4641(13)	2.474(2)	2.4740(12)
Ir1–N1	2.161(7)	2.163(4)	2.157(4)	2.163(3)	2.144(4)	2.147(6)	2.174(4)
Ir1–N2	2.110(7)	2.097(4)	2.106(4)	2.107(4)	2.100(4)	2.113(6)	2.115(4)
C1–C2	1.340(12)	1.349(7)	1.349(7)	1.359(6)	1.368(6)	1.343(11)	1.349(6)
C2–C3	1.480(11)	1.477(6)	1.477(6)	1.470(6)	1.467(7)	1.477(11)	1.466(7)
C3–C4	1.410(12)	1.419(6)	1.422(7)	1.431(5)	1.423(7)	1.430(11)	1.383(7)
C1–Ir1–C4	79.9(3)	80.43(18)	80.31(19)	80.83(16)	80.4(2)	80.5(3)	80.08(19)
C2–C1–Ir1	116.9(6)	117.0(3)	116.8(3)	116.8(3)	116.9(4)	117.2(6)	116.6(4)
C1–C2–C3	115.5(7)	115.4(4)	115.5(4)	115.5(4)	114.9(4)	115.0(7)	113.4(4)
C2–C3–C4	112.1(7)	112.8(4)	112.4(4)	112.7(3)	113.0(4)	112.4(7)	115.8(4)
C3–C4–Ir1	115.5(5)	114.2(3)	114.6(3)	114.0(3)	114.5(4)	114.1(5)	113.8(4)

Figure 4. Molecular structures of (a) 4, (b) 5, (c) 6, (d) 8, (e) 9, (f) 10, and (g) 12 (50% probability thermal ellipsoids). The counteranion and phenyl moieties in PPh₃ are omitted for clarity.Table 2. Photophysical Data of 4–12 in Deaerated CH₂Cl₂ at RT as Well as Their Experimentally Measured Radiative and Nonradiative Rate Constants

compound	λ_{em} (nm)	Φ_{PL}^a	τ (ns) ^a	k_r (10 ⁵ s ⁻¹) ^b	k_{nr} (10 ⁵ s ⁻¹) ^b
4	559	45%	582	0.77	0.95
5	551	48%	421	1.1	1.2
6	615	9.6%	104	0.93	8.7
7	561	32%	315	1.0	2.2
8	551	64%	495	1.3	0.7
9	535	40%	405	1.0	1.5
10	555	39%	360	1.1	1.7
11	549	24%	269	0.90	2.8
12	642	<1%	138	<0.1	7.2

^a Φ_{PL} and τ were measured on an Edinburgh FLS980 spectrophotometer equipped with an integrating sphere at RT. ^bParameters k_r and k_{nr} were calculated according to the equations $k_r = \Phi_{PL}/\tau$ and $k_{nr} = (1 - \Phi_{PL})/\tau$.

in Table 2. All compounds have high k_r values, except for 12, which may be attributed to the strong spin–orbit coupling of the iridium core and thus promote the fast energy transfer from the singlet to the triplet state.^{8a,10f} In addition, the values of k_{nr} for 6, 7, 11, and 12 are obviously larger than those of other compounds. We inferred that the relatively narrow energy gaps between HOMO and LUMO of 6 and 12 might be responsible

for their extremely high k_{nr} values, which are in good agreement with the energy gap law.¹⁸ Previous report demonstrated that the sulfur atom in the ligands can considerably deteriorate the Φ_{PL} of the Ir(III) complexes,^{18b} which can explain the low Φ_{PL} and k_r value of 12. The increasing vibrational freedom of the methoxyl substituted compounds 7 and 11 can be attributed to a subtle balance of their abnormal Φ_{PL} , τ , and k_{nr} .^{18b} However, the complexity of the interaction prevents us from achieving a thorough understanding of the balance.

Figure 5 displays the UV–vis absorption and normalized emission spectra of iridapolycycles 3–12. To ensure the accurate comparisons, the previously reported compound 3¹³ was redetermined under the same conditions. The maximum emission wavelength of 3 was confirmed to be 580 nm. As shown in Figure 5a,c, all these iridapolycycles have intense absorption bands below $\lambda = 350$ nm, which can be assigned to spin-allowed $\pi \rightarrow \pi^*$ intraligand transitions. The weak absorption bands from 350 to 580 nm, greatly depending on the structures, are attributed to a combination of MLCT and LLCT.¹⁹ The absorption peaks of compounds 6, 9, 11, and 12 were further investigated in wavelength region between 460 to 540 nm. TD-DFT calculations (Table S2) demonstrated that the 500 nm centered adsorption bands of the compounds is closely related to the transition from HOMO–1 to LUMO, which can also be attributed to MLCT/LLCT character.

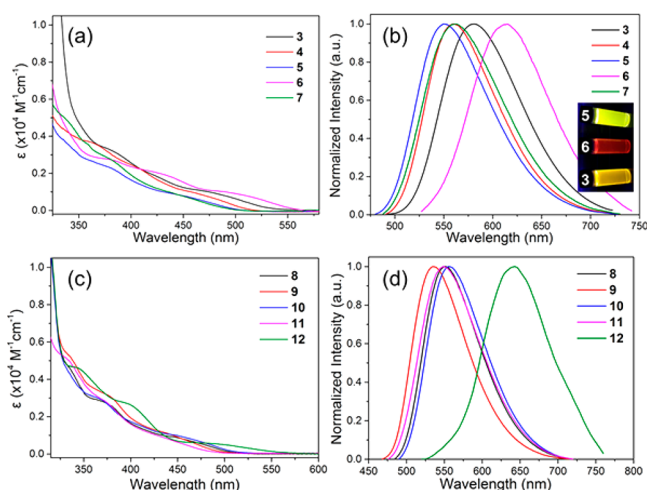


Figure 5. (a) Absorption spectra and (b) normalized emission spectra of 3–7 in CH_2Cl_2 at RT; (c) absorption spectra and (d) normalized emission spectra of 8–12 in CH_2Cl_2 at RT.

In accordance with the computational results, the λ_{em} of compound 4 bearing a 1,10-phenanthroline ligand exhibits a 20 nm blueshift when compared with that of 3. The electron-donating substituents on the N[^]N unit of 5 lead to blue-shift effects on their emission color, while the λ_{em} of 6 is significantly red-shifted by the aid of electron-withdrawing group on the N[^]N unit (Table 2, Figure 5b).

The experimental results for 8, 10, and 12 are also in line with theoretical calculations. The λ_{em} of iridapolycycles 8, 10, and 12 are 551, 555, and 642 nm, suggesting the efficient color modulation. The electron-withdrawing groups on the C[^]C unit indeed can trigger a blueshift, while the replacement of benzene ring by thiophene ring in the C[^]C unit of 12 resulted in a dramatic redshift from 580 to 642 nm (Table 2, Figure 5d). Compared to the emission of 2-thieno,¹³ introducing a rigid N[^]N ligand in 12 induces a 20 nm redshift of emission maximum and a slight emission enhancement (Figure 6).

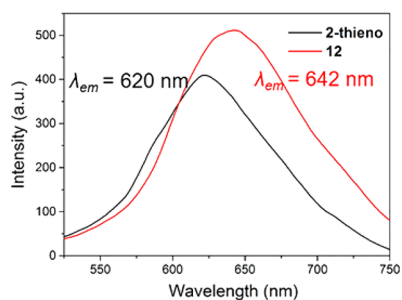


Figure 6. Emission spectra (1.0×10^{-4} mol/L) of 2-thieno and 12 in CH_2Cl_2 at RT.

It is noteworthy that the emission of 9 shifts to 535 nm in the green region (Table 2, Figure 5d), which can be assigned to the combined effect of two electron-donating *tert*-butyl groups in the N[^]N unit and one electron-withdrawing bromine atom in the C[^]C unit. Both the frontier orbital distribution and the electronic effects of the substituent groups are important for the emission shift. Grafting an electron-withdrawing group onto the C[^]C unit would decrease the σ donation of the ligand as well as the electron density of iridium center, thus generate a stabilized

HOMO,^{9a} while the electron-donating group of the N[^]N part would lead to a destabilized LUMO.^{18b}

The measured wavelength shifts in λ_{em} of these compounds are in good agreement with the DFT-calculated trends of the ΔE_s . The spectra clearly show that the tuning effect could be further enhanced by the synergy of modifications on both the C[^]C and N[^]N units. We noticed that compounds 7 and 11 bearing methoxyl groups have the largest ΔE_s among the calculated iridapolycycle models; however, these present abnormal emission wavelengths ($\lambda_{\text{em}} = 561$ and 549 nm) compared to that of 9 ($\lambda_{\text{em}} = 535$ nm). The blue-shifted adsorption bands in compounds 7 and 11 (Figures 5a,c) are consistent with the trend of their energy bandgaps, while their emission maxima (Table 2) are not fully compatible with the energy levels of T₁ (Table S2) and the ΔE_s (Figure 3). Although the electron-donating effect of methoxyl groups on N[^]N unit of 7 and 11 appear to be diminished when they are photon-excited, the synergetic modification on both C[^]C and N[^]N units is evident in compound 11 compared to compounds 7 and 3.

CONCLUSION

We developed a convenient method for the emission color modulation of iridapolycycles $[(\text{N}^{\wedge}\text{N})\text{Ir}(\text{C}^{\wedge}\text{C})\text{Cl}(\text{PPh}_3)]^+$. Our experimental results support the theoretically deduced conclusion that the color modulation of the emitted light primarily depends on the structural modifications on the N[^]N ligands and the C[^]C frameworks. On the basis of satisfactory performance in luminescence, we expect that this method would provide a predictable and precise color-tuning strategy for promisingly achieving phosphorescent devices with iridapolycycles architecture. The investigation paves the way for exploiting iridacycles with metal core embedded in the all-carbon rings in the field of luminescent materials.

EXPERIMENTAL SECTION

Syntheses and Materials. All manipulations were performed at room temperature under a nitrogen atmosphere using standard Schlenk techniques unless otherwise stated. Solvents were distilled from sodium/benzophenone (diethyl ether) or calcium hydride (DCM) under N_2 prior to use. Other reagents were used as received from commercial sources without further purification.

General Methods. NMR spectroscopic experiments were performed on Bruker Avance III 850 MHz spectrometer, Bruker Avance III 500 MHz and Bruker Avance II 400 MHz. The ^1H and ^{13}C NMR chemical shifts shown are relative to TMS, and the ^{31}P NMR chemical shifts shown are relative to 85% H_3PO_4 . Elemental analyses were performed on an Elementar Vario EL III elemental analyzer. UV–visible absorption spectra were recorded using a Hitachi U-3900 ultraviolet–visible spectrophotometer and fluorescence spectra were measured with a Hitachi F-7400 fluorophotometer. Luminescent lifetimes and absolute quantum yields were measured on an Edinburgh FLS 980 spectrophotometer equipped with an integrating sphere in room temperature.

Theoretical Calculations. The DFT and TD-DFT calculations were performed using the Gaussian 09 suite of programs,¹⁴ and the LANL2DZ basis set¹⁵ was used to treat the Ir, P, Br, S, and Cl atoms, whereas the 6-31G basis set was used to treat all other atoms.

Preparation of 1-Br. 1-Bromo-4-ethynylbenzene (87 mg, 0.48 mmol) and PPh_3 (346 mg, 1.32 mmol) were added to a solution of $[\text{IrH}(\text{CO})\text{Cl}(\text{PPh}_3)_3]\text{BF}_4$ (500 mg, 0.44 mmol) in chloroform (10 mL). The mixture was stirred in N_2 at room temperature for 3 h to give a clear solution. The solvent was removed under vacuum, and the addition of diethyl ether (3×10 mL) to the residue produced 1-Br as a white solid (534 mg, 92%). ^1H NMR (400.0 MHz, CDCl_3): $\delta = 10.2$

(d, $^3J_{\text{PH}} = 36.9$ Hz, 1H, IrCH), 5.8–7.9 (m, 49H, PPh₃ and phenyl), –8.3 (td, $^2J_{\text{PH}} = 16.2$ Hz, $^4J_{\text{PH}} = 14.8$ Hz, 1H, IrH). ^{31}P NMR (161.9 MHz, CDCl₃): $\delta = 19.9$ (s, CPh₃), –1.0 (s, IrPPh₃). ^{13}C NMR (100.6 MHz, CDCl₃): $\delta = 187.4$ (m, IrCH), 164.2 (t, $^2J_{\text{PC}} = 7.2$ Hz, CO), 118.0–137.0 (m, PPh₃ and Phenyl), 121.9 (d, $^1J_{\text{PC}} = 58.4$ Hz, IrCHC(PPh₃)). Anal. Calcd for C₆₃H₅₁BBrClF₄IrOP₃: C 57.70, H 3.92. Found: C 57.43, H 3.77.

Preparation of 1-F. 1-Ethynyl-4-fluorobenzene (58 mg, 0.48 mmol) and PPh₃ (346 mg, 1.32 mmol) were added to a solution of [IrH(CO)Cl(PPh₃)₃]BF₄ (500 mg, 0.44 mmol) in chloroform (10 mL). The mixture was stirred in N₂ at room temperature for 3 h to give a clear solution. The solvent was removed under vacuum, and the addition of diethyl ether (3 × 10 mL) to the residue produced 1-F as a white solid (470 mg, 85%). ^1H NMR (400.0 MHz, CDCl₃): $\delta = 10.2$ (d, $^3J_{\text{PH}} = 36.3$ Hz, 1H, IrCH), 6.0–7.8 (m, 49H, PPh₃ and phenyl), –8.2 (td, $^2J_{\text{PH}} = 16.2$ Hz, $^4J_{\text{PH}} = 15.3$ Hz, 1H, IrH). ^{31}P NMR (161.9 MHz, CDCl₃): $\delta = 19.8$ (s, CPh₃), –1.0 (s, IrPPh₃). ^{13}C NMR (100.6 MHz, CDCl₃): $\delta = 187.8$ (m, IrCH), 163.7 (d, $^2J_{\text{PC}} = 250.4$ Hz, CF), 163.6 (t, $^2J_{\text{PC}} = 7.1$ Hz, CO), 115.4–134.8 (m, PPh₃ and Phenyl), 121.2 (d, $^1J_{\text{PC}} = 57.4$ Hz, IrCHC(PPh₃)). Anal. Calcd for C₆₃H₅₁BClF₃IrOP₃: C 60.51, H 4.11. Found: C 60.74, H 4.35.

Preparation of 4. 1,10-Phenanthroline (108 mg, 0.60 mmol), sodium hexafluorophosphate (120 mg, 0.71 mmol), and trimethylamine oxide (60 mg, 0.80 mmol) were added to a solution of 1 (150 mg, 0.12 mmol) in chloroform (10 mL). The mixture was refluxed for about 72 h in nitrogen atmosphere. The solution was then concentrated to approximately 1 mL under vacuum. Addition of diethyl ether (10 mL) to the solution gave a yellow precipitate. After filtration, the crude product was subjected to column chromatography (alumina gel; eluted with dichloromethane/acetone, 30:1 v/v). Compound 4 was obtained as a light-yellow solid (87 mg, 61%). ^1H NMR (400.0 MHz, CD₂Cl₂): $\delta = 10.1$ (d, $^3J_{\text{PH}} = 19.9$ Hz, 1H, IrCH), 8.0–9.3 (m, 6H, 1,10-phenanthroline), 7.1–8.0 (m, 30H, PPh₃; 2H, 1,10-phenanthroline), 5.2–6.4 (m, 4H, phenyl). ^{31}P NMR (202.5 MHz, CD₂Cl₂): $\delta = 11.7$ (s, CPh₃), –10.1 (s, IrPPh₃), –144.5 (quint, $^1J_{\text{PF}} = 708.5$ Hz, PF₆). ^{13}C NMR (100.6 MHz, CD₂Cl₂): $\delta = 191.8$ (d, $^2J_{\text{PC}} = 9.6$ Hz, IrCH), 152.5, 151.9, 149.2, 149.1, 146.8, 146.2 (s, 1,10-phenanthroline), 151.4 (d, $^2J_{\text{PC}} = 19.6$ Hz, IrCHC(PPh₃)C), 144.8 (dd, $^2J_{\text{PC}} = 18.8$ Hz, $^3J_{\text{PC}} = 6.4$ Hz, IrC), 120.9–137.7 (m, PPh₃, phenyl, and 1,10-phenanthroline), 118.9 (d, $^1J_{\text{PC}} = 87.9$ Hz, IrCHC(PPh₃)). Anal. Calcd for C₅₆H₄₃ClF₆IrN₂P₃: C 57.07, H 3.68, N 2.38. Found: C 57.16, H 4.05, N 2.21.

Preparation of 5. 4,4'-Di-*tert*-butyl-2,2'-bipyridine (160 mg, 0.60 mmol), sodium hexafluorophosphate (120 mg, 0.71 mmol), and trimethylamine oxide (60 mg, 0.80 mmol) were added to a solution of 1 (150 mg, 0.12 mmol) in chloroform (10 mL). The mixture was refluxed for about 72 h in nitrogen atmosphere. The solution was then concentrated to approximately 1 mL under vacuum. Addition of *n*-hexane (10 mL) to the solution gave a yellow-green precipitate. After filtration, the crude product was subjected to column chromatography (alumina gel; eluted with dichloromethane/acetone, 50:1 v/v). Compound 5 was obtained as a yellow-green solid (72 mg, 47%). ^1H NMR (500.2 MHz, CDCl₃): $\delta = 9.9$ (d, $^3J_{\text{PH}} = 20.2$ Hz, 1H, IrCH), 8.0–8.8 (m, 4H, bipyridyl), 7.0–7.9 (m, 30H, PPh₃; 2H, bipyridyl), 5.3–6.5 (m, 4H, phenyl), 1.3–1.5 (s, 18H, *tert*-butyl). ^1H NMR (500.2 MHz, CDCl₃): $\delta = 9.9$ (d, $^3J_{\text{PH}} = 20.2$ Hz, 1H, IrCH), 8.0–8.8 (m, 4H, bipyridyl), 7.0–7.9 (m, 30H, PPh₃; 2H, bipyridyl), 5.3–6.5 (m, 4H, phenyl), 1.3–1.5 (s, 18H, *tert*-butyl). ^{13}C NMR (125.8 MHz, CDCl₃): $\delta = 193.7$ (d, $^2J_{\text{PC}} = 10.1$ Hz, IrCH), 163.8 (d, $^2J_{\text{PC}} = 27.4$ Hz, IrCHC(PPh₃)C), 156.3, 155.9, 152.6, 152.4, 149.6 (s, bipyridyl), 145.0 (dd, $^2J_{\text{PC}} = 19.0$ Hz, $^3J_{\text{PC}} = 6.8$ Hz, IrC), 120.0–134.7 (m, PPh₃, phenyl, and bipyridyl), 120.0 (d, $^1J_{\text{PC}} = 85.3$ Hz, IrCHC(PPh₃)), 35.6, 35.5, 30.4, 30.3 (s, *tert*-butyl). Anal. Calcd for C₆₂H₅₉ClF₆IrN₂P₃: C 58.79, H 4.69, N 2.21, found: C 58.54, H 4.38, N 2.32.

Preparation of 6. 4,4'-Dibromo-2,2'-bipyridine (187 mg, 0.60 mmol), sodium hexafluorophosphate (120 mg, 0.71 mmol), and trimethylamine oxide (60 mg, 0.80 mmol) were added to a solution of 1 (150 mg, 0.12 mmol) in chloroform (10 mL). The mixture was refluxed for about 72 h in nitrogen atmosphere. The solution was then concentrated to approximately 1 mL under vacuum. Addition of

diethyl ether (10 mL) to the solution gave a light-red precipitate. After filtration, the crude product was subjected to column chromatography (alumina gel; eluted with dichloromethane/acetone, 20:1 v/v). Compound 6 was obtained as a red solid (56 mg, 35%). ^1H NMR (400.0 MHz, CD₂Cl₂): $\delta = 9.7$ (d, $^3J_{\text{PH}} = 20.3$ Hz, 1H, IrCH), 8.1–8.6 (m, 4H, bipyridyl), 7.0–7.8 (m, 30H, PPh₃; 2H, bipyridyl), 5.2–6.4 (m, 4H, phenyl). ^{31}P NMR (161.0 MHz, CD₂Cl₂): $\delta = 11.8$ (s, CPh₃), –10.4 (s, IrPPh₃), –144.5 (quint, $^1J_{\text{PF}} = 712.7$ Hz, PF₆). ^{13}C NMR (100.6 MHz, CD₂Cl₂): $\delta = 190.3$ (d, $^2J_{\text{PC}} = 9.7$ Hz, IrCH), 155.3 (d, $^2J_{\text{PC}} = 32.1$ Hz, IrCHC(PPh₃)C), 152.2, 151.4, 151.2, 149.6 (s, bipyridyl), 144.6 (dd, $^2J_{\text{PC}} = 18.6$ Hz, $^3J_{\text{PC}} = 6.7$ Hz, IrC), 121.4–135.7 (m, PPh₃, phenyl, and bipyridyl), 118.8 (d, $^1J_{\text{PC}} = 85.3$ Hz, IrCHC(PPh₃)). Anal. Calcd for C₅₄H₄₁Br₂ClF₆IrN₂P₃: C 49.42, H 3.15, N 2.13. Found: C 49.07, H 2.85, N 1.97.

Preparation of 7. 4,4'-Dimethoxy-2,2'-bipyridine (130 mg, 0.60 mmol), sodium hexafluorophosphate (120 mg, 0.71 mmol), and trimethylamine oxide (60 mg, 0.80 mmol) were added to a solution of 1 (150 mg, 0.12 mmol) in chloroform (10 mL). The mixture was refluxed for about 72 h in nitrogen atmosphere. The solution was then concentrated to approximately 1 mL under vacuum. Addition of diethyl ether (10 mL) to the solution gave a yellow precipitate. After filtration, the crude product was subjected to column chromatography (alumina gel; eluted with dichloromethane/acetone, 50:1 v/v). Compound 7 was obtained as a yellow-green solid (77 mg, 52%). ^1H NMR (400.0 MHz, CD₂Cl₂): $\delta = 9.8$ (d, $^3J_{\text{PH}} = 19.4$ Hz, 1H, IrCH), 8.0–8.6 (m, 2H, bipyridyl), 6.7–7.8 (m, 30H, PPh₃; 4H, bipyridyl), 5.3–6.3 (m, 4H, phenyl), 3.8–4.0 (s, 6H, dimethoxy). ^{31}P NMR (161.9 MHz, CD₂Cl₂): $\delta = 11.6$ (s, CPh₃), –9.6 (s, IrPPh₃), –144.5 (quint, $^1J_{\text{PF}} = 705.6$ Hz, PF₆). ^{13}C NMR (100.6 MHz, CD₂Cl₂): $\delta = 193.1$ (d, $^2J_{\text{PC}} = 9.3$ Hz, IrCH), 166.9, 166.5, 157.0, 156.6, 153.1, 150.0 (s, bipyridyl), 151.7 (d, $^2J_{\text{PC}} = 20.2$ Hz, IrCHC(PPh₃)C), 145.4 (dd, $^2J_{\text{PC}} = 19.5$ Hz, $^3J_{\text{PC}} = 5.6$ Hz, IrC), 109.1–133.7 (m, PPh₃, phenyl, and bipyridyl), 119.5 (d, $^1J_{\text{PC}} = 87.7$ Hz, IrCHC(PPh₃)), 56.0, 55.9 (s, dimethoxy). Anal. Calcd for C₅₆H₄₇ClF₆IrN₂O₂P₃: C 55.38, H 3.90, N 2.31. Found: C 55.20, H 4.09, N 2.34.

Preparation of 8. 2,2'-Bipyridine (94 mg, 0.60 mmol), sodium hexafluorophosphate (120 mg, 0.71 mmol), and trimethylamine oxide (60 mg, 0.80 mmol) were added to a solution of 1-Br (160 mg, 0.12 mmol) in chloroform (10 mL). The mixture was refluxed for about 72 h in nitrogen atmosphere. The solution was then concentrated to approximately 1 mL under vacuum. Addition of diethyl ether (10 mL) to the solution gave a light-yellow precipitate. After filtration, the crude product was subjected to column chromatography (alumina gel; eluted with dichloromethane/acetone, 20:1 v/v). Compound 8 was obtained as a yellow solid (83 mg, 55%). ^1H NMR (500.2 MHz, CDCl₃): $\delta = 10.0$ (d, $^3J_{\text{PH}} = 21.6$ Hz, 1H, IrCH), 8.0–8.9 (m, 6H, bipyridyl), 7.1–7.9 (m, 30H, PPh₃; 2H, bipyridyl), 5.2–6.5 (m, 3H, phenyl). ^{31}P NMR (202.5 MHz, CDCl₃): $\delta = 11.5$ (s, CPh₃), –10.8 (s, IrPPh₃), –144.5 (quint, $^1J_{\text{PF}} = 712.3$ Hz, PF₆). ^{13}C NMR (125.8 MHz, CDCl₃): $\delta = 193.2$ (d, $^2J_{\text{PC}} = 9.6$ Hz, IrCH), 156.4, 155.7, 152.4, 152.3, 149.7 (s, bipyridyl), 151.3 (d, $^2J_{\text{PC}} = 20.0$ Hz, IrCHC(PPh₃)C), 148.6 (dd, $^2J_{\text{PC}} = 18.5$ Hz, $^3J_{\text{PC}} = 6.4$ Hz, IrC), 122.9–140.0 (m, PPh₃, phenyl, and bipyridyl), 119.3 (d, $^1J_{\text{PC}} = 87.6$ Hz, IrCHC(PPh₃)). Anal. Calcd for C₅₄H₄₂BrClF₆IrN₂P₃: C 52.58, H 3.43, N 2.27. Found: C 52.2, H 3.13, N 1.91.

Preparation of 9. 4,4'-Di-*tert*-butyl-2,2'-bipyridine (160 mg, 0.60 mmol), sodium hexafluorophosphate (120 mg, 0.71 mmol), and trimethylamine oxide (60 mg, 0.80 mmol) were added to a solution of 1-Br (160 mg, 0.12 mmol) in chloroform (10 mL). The mixture was refluxed for about 72 h in nitrogen atmosphere. The solution was then concentrated to approximately 1 mL under vacuum. Addition of *n*-hexane (10 mL) to the solution gave a yellow-green precipitate. After filtration, the crude product was subjected to column chromatography (alumina gel; eluted with dichloromethane/acetone, 50:1 v/v). Compound 9 was obtained as a yellow-green solid (51 mg, 31%). ^1H NMR (400.0 MHz, CD₂Cl₂): $\delta = 9.9$ (d, $^3J_{\text{PH}} = 20.2$ Hz, 1H, IrCH), 8.0–8.7 (m, 4H, bipyridyl), 7.0–7.9 (m, 30H, PPh₃; 2H, bipyridyl), 5.1–6.5 (m, 3H, phenyl), 1.3–1.4 (s, 18H, *tert*-butyl). ^{31}P NMR (161.9 MHz, CD₂Cl₂): $\delta = 11.8$ (s, CPh₃), –10.2 (s, IrPPh₃),

−144.4 (quint, $^1J_{PF} = 711.0$ Hz, PF_6). ^{13}C NMR (100.6 MHz, CD_2Cl_2): $\delta = 193.2$ (d, $^2J_{PC} = 9.8$ Hz, IrCH), 163.3 (d, $^2J_{PC} = 20.0$ Hz, IrCHC(PPh_3)C), 155.4, 155.0, 151.5, 151.0, 148.7 (s, bipyridyl), 148.4 (dd, $^2J_{PC} = 18.9$ Hz, $^3J_{PC} = 6.3$ Hz, IrC), 120.0–134.7 (m, PPh_3 , phenyl, and bipyridyl), 118.5 (d, $^1J_{PC} = 88.0$ Hz, IrCHC(PPh_3)), 34.8, 29.3 (m, *tert*-butyl). Anal. Calcd for $C_{62}H_{58}BrClF_6IrN_2P_3$: C 55.34, H 4.34, N 2.08. Found: C 55.51, H 4.37, N 2.21.

Preparation of 10. 2,2'-Bipyridine (94 mg, 0.60 mmol), sodium hexafluorophosphate (120 mg, 0.71 mmol), and trimethylamine oxide (60 mg, 0.80 mmol) were added to a solution of 1-F (150 mg, 0.12 mmol) in chloroform (10 mL). The mixture was refluxed for about 72 h in nitrogen atmosphere. The solution was then concentrated to approximately 1 mL under vacuum. Addition of diethyl ether (10 mL) to the solution gave a yellow precipitate. After filtration, the crude product was subjected to column chromatography (alumina gel; eluted with dichloromethane/acetone, 20:1 v/v). Compound 10 was obtained as a yellow solid (60 mg, 43%). 1H NMR (400.0 MHz, CD_2Cl_2): $\delta = 9.8$ (d, $^3J_{PH} = 19.7$ Hz, 1H, IrCH), 7.9–8.7 (m, 6H, bipyridyl), 7.0–7.8 (m, 30H, PPh_3 ; 2H, bipyridyl), 4.8–6.3 (m, 3H, phenyl). ^{31}P NMR (161.9 MHz, CD_2Cl_2): $\delta = 11.6$ (s, $CPPh_3$), −10.6 (s, $IrPPh_3$), −144.5 (quint, $^1J_{PF} = 709.1$ Hz, PF_6). ^{13}C NMR (100.6 MHz, CD_2Cl_2): $\delta = 190.3$ (d, $^2J_{PC} = 9.7$ Hz, IrCH), 160.7, 158.2, 155.5, 155.1, 151.8, 149.1 (s, bipyridyl), 149.3 (dd, $^2J_{PC} = 19.6$ Hz, $^3J_{PC} = 5.1$ Hz, IrC), 148.0 (d, $^2J_{PC} = 19.2$ Hz, IrCHC(PPh_3)C), 107.0–138.8 (m, PPh_3 , phenyl, and bipyridyl), 119.1 (d, $^1J_{PC} = 87.4$ Hz, IrCHC(PPh_3)). Anal. Calcd for $C_{54}H_{42}ClF_7IrN_2P_3$: C 55.32, H 3.61, N 2.39. Found: C 55.28, H 3.31, N 2.20.

Preparation of 11. 4,4'-Dimethoxy-2,2'-bipyridine (130 mg, 0.60 mmol), sodium hexafluorophosphate (120 mg, 0.71 mmol) and trimethylamine oxide (60 mg, 0.80 mmol) were added to a solution of 1-F (150 mg, 0.12 mmol) in chloroform (10 mL). The mixture was refluxed for about 72 h in nitrogen atmosphere. The solution was then concentrated to approximately 1 mL under vacuum. Addition of diethyl ether (10 mL) to the solution gave a yellow-green precipitate. After filtration, the crude product was subjected to column chromatography (alumina gel; eluted with dichloromethane/acetone, 50:1 v/v). Compound 11 was obtained as a yellow-green solid (70 mg, 47%). 1H NMR (400.0 MHz, CD_2Cl_2): $\delta = 9.7$ (d, $^3J_{PH} = 20.3$ Hz, 1H, IrCH), 8.0–8.6 (m, 2H, bipyridyl), 6.7–7.8 (m, 30H, PPh_3 ; 4H, bipyridyl), 4.9–6.2 (m, 3H, phenyl), 3.9–4.0 (s, 6H, dimethoxy). ^{31}P NMR (161.9 MHz, CD_2Cl_2): $\delta = 11.7$ (s, $CPPh_3$), −10.0 (s, $IrPPh_3$), −144.4 (quint, $^1J_{PF} = 711.1$ Hz, PF_6). ^{13}C NMR (100.6 MHz, CD_2Cl_2): $\delta = 191.1$ (d, $^2J_{PC} = 9.3$ Hz, IrCH), 167.0, 166.7, 160.6, 158.1, 157.0, 156.5, 153.0, 150.0 (s, bipyridyl), 149.3 (dd, $^2J_{PC} = 19.6$ Hz, $^3J_{PC} = 5.1$ Hz, IrC), 148.0 (d, $^2J_{PC} = 19.2$ Hz, IrCHC(PPh_3)C), 106.8–133.9 (m, PPh_3 , phenyl, and bipyridyl), 118.8 (d, $^1J_{PC} = 87.8$ Hz, IrCHC(PPh_3)), 56.1, 56.0 (s, dimethoxy). Anal. Calcd for $C_{56}H_{46}ClF_7IrN_2O_2P_3$: C 54.57, H 3.76, N 2.27. Found: C 54.92, H 4.05, N 2.24.

Preparation of 12. 2,2'-Bipyridyl (135 mg, 0.86 mmol) and sodium hexafluorophosphate (170 mg, 1.01 mmol) were added to a solution of 2-thieno (200 mg, 0.17 mmol) in chloroform (15 mL). The mixture was heated in N_2 under reflux in a Schlenk tube for about 48 h. The solution was then concentrated to approximately 1 mL under vacuum. Addition of diethyl ether (10 mL) to the solution gave a red precipitate. After filtration, the crude product was subjected to column chromatography (alumina gel; eluted with dichloromethane/acetone, 30:1 v/v). Compound 12 was obtained as a red solid (64 mg, 32%). 1H NMR (400.0 MHz, CD_2Cl_2): $\delta = 9.8$ (d, $^3J_{PH} = 18.9$ Hz, 1H, IrCH), 7.9–8.8 (m, 6H, bipyridyl), 7.1–7.9 (m, 30H, PPh_3 ; 2H, bipyridyl), 6.6 (d, $^3J_{HH} = 4.7$ Hz, 1H, SCH), 5.1 (d, $^3J_{HH} = 4.4$ Hz, 1H, SCHCH). ^{31}P NMR (161.9 MHz, CD_2Cl_2): $\delta = 9.5$ (s, $CPPh_3$), −11.5 (s, $IrPPh_3$), −144.5 (quint, $^1J_{PF} = 712.1$ Hz, PF_6). ^{13}C NMR (100.6 MHz, CD_2Cl_2): $\delta = 184.1$ (d, $^2J_{PC} = 10.0$ Hz, IrCH), 155.8, 155.2, 152.1, 150.0 (s, bipyridyl), 141.4 (dd, $^2J_{PC} = 18.7$ Hz, $^3J_{PC} = 6.5$ Hz, IrC), 141.0 (d, $^2J_{PC} = 19.8$ Hz, IrCHC(PPh_3)C), 123.4–134.0 (m, PPh_3 , phenyl, and bipyridyl), 122.6 (s, SCHCH), 119.6 (s, SCH), 118.3 (d, $^1J_{PC} = 88.4$ Hz, IrCHC(PPh_3)). Anal. Calcd for $C_{52}H_{41}ClF_6IrN_2P_3S$: C 53.82, H 3.56, N 2.41. Found: C 53.51, H 3.43, N 2.38.

Crystallographic Details. Single-crystal X-ray diffraction data were collected on an Oxford Gemini S Ultra or a Rigaku R-Axis SPIDER IP CCD area detector using graphite-monochromated Mo $K\alpha$ radiation ($\lambda = 0.71073$ Å). Multiscan absorption corrections (SADABS) were applied. Using Olex2, the structure was solved with the ShelXT structure solution program using Direct Methods and refined with the ShelXL refinement package using Least Squares minimization. All non-H atoms were refined anisotropically unless otherwise stated. Hydrogen atoms were placed at idealized positions and refined as riding atoms unless otherwise stated. Further details on crystal data, data collection, and refinements are summarized in Table S1. CCDC 1473807–1473813 contain the supplementary crystallographic data for this paper. These data can be obtained free of charge from The Cambridge Crystallographic Data Center via www.ccdc.cam.ac.uk/data_request/cif.

■ ASSOCIATED CONTENT

● Supporting Information

The Supporting Information is available free of charge on the ACS Publications website at DOI: 10.1021/acs.organomet.7b00699.

NMR spectra and theoretical calculations data of 4–12 (PDF)

Cartesian coordinates of 3'–15' (XYZ)

■ Accession Codes

CCDC 1473807–1473813 contain the supplementary crystallographic data for this paper. These data can be obtained free of charge via www.ccdc.cam.ac.uk/data_request/cif, or by emailing data_request@ccdc.cam.ac.uk, or by contacting The Cambridge Crystallographic Data Centre, 12 Union Road, Cambridge CB2 1EZ, UK; fax: +44 1223 336033.

■ AUTHOR INFORMATION

■ Corresponding Author

*E-mail: zh@xmu.edu.cn.

■ ORCID

Hong Zhang: 0000-0003-3010-0806

Zhenyang Lin: 0000-0003-4104-8767

■ Notes

The authors declare no competing financial interest.

■ ACKNOWLEDGMENTS

We thank the NSFC (21572185 and 21561162001), the Research Grants Council of Hong Kong (N_HKUST603/15), and the Fundamental Research Funds for the Central Universities (20720150046).

■ REFERENCES

- (a) Guo, K.; Wang, H.; Wang, Z.; Si, C.; Peng, C.; Chen, G.; Zhang, J.; Wang, G.; Wei, B. *Chem. Sci.* **2017**, *8*, 1259–1268. (b) Kuei, C.-Y.; Tsai, W.-L.; Tong, B.; Jiao, M.; Lee, W.-K.; Chi, Y.; Wu, C.-C.; Liu, S.-H.; Lee, G.-H.; Chou, P.-T. *Adv. Mater.* **2016**, *28*, 2795–2800. (c) Kesarkar, S.; Mróz, W.; Penconi, M.; Pasini, M.; Destri, S.; Cazzaniga, M.; Ceresoli, D.; Mussini, P. R.; Baldoli, C.; Giovannella, U.; Bossi, A. *Angew. Chem., Int. Ed.* **2016**, *55*, 2714–2718. (d) Tao, P.; Li, W.-L.; Zhang, J.; Guo, S.; Zhao, Q.; Wang, H.; Wei, B.; Liu, S.-J.; Zhou, X.-H.; Yu, Q.; Xu, B.-S.; Huang, W. *Adv. Funct. Mater.* **2016**, *26*, 881–894. (e) Jurow, M. J.; Mayr, C.; Schmidt, T. D.; Lampe, T.; Djurovich, P. I.; Brütting, W.; Thompson, M. E. *Nat. Mater.* **2015**, *15*, 85–91.
- (a) Jiang, X.; Peng, J.; Wang, J.; Guo, X.; Zhao, D.; Ma, Y. *ACS Appl. Mater. Interfaces* **2016**, *8*, 3591–3600. (b) Guo, S.; Ma, Y.; Liu, S.; Yu, Q.; Xu, A.; Han, J.; Wei, L.; Zhao, Q.; Huang, W. *J. Mater. Chem. C* **2016**, *4*, 6110–6116. (c) Bejormohandas, K. S.; Kumar, A.;

- Sreenadh, S.; Varathan, E.; Varughese, S.; Subramanian, V.; Reddy, M. L. P. *Inorg. Chem.* **2016**, *55*, 3448–3461. (d) Wang, W.; Mao, Z.; Wang, M.; Liu, L.-J.; Kwong, D. W. J.; Leung, C.-H.; Ma, D.-L. *Chem. Commun.* **2016**, *52*, 3611–3614. (e) Ryu, S. Y.; Huh, M.; You, Y.; Nam, W. *Inorg. Chem.* **2015**, *54*, 9704–9714.
- (3) (a) Liu, C.; Yang, C.; Lu, L.; Wang, W.; Tan, W.; Leung, C.-H.; Ma, D.-L. *Chem. Commun.* **2017**, *53*, 2822–2825. (b) Tang, T. S.-M.; Liu, H.-W.; Lo, K. K.-W. *Chem. Commun.* **2017**, *53*, 3299–3302. (c) Lee, L. C.-C.; Lau, J. C.-W.; Liu, H.-W.; Lo, K. K.-W. *Angew. Chem., Int. Ed.* **2016**, *55*, 1046–1049. (d) Wang, M.; Mao, Z.; Kang, T.-S.; Wong, C.-Y.; Mergny, J.-L.; Leung, C.-H.; Ma, D.-L. *Chem. Sci.* **2016**, *7*, 2516–2523. (e) Sun, L.; Chen, Y.; Kuang, S.; Li, G.; Guan, R.; Liu, J.; Ji, L.; Chao, H. *Chem. - Eur. J.* **2016**, *22*, 8955–8965.
- (4) (a) Genoni, A.; Chiridon, D. N.; Boniolo, M.; Sartorel, A.; Bernhard, S.; Bonchio, M. *ACS Catal.* **2017**, *7*, 154–160. (b) Yang, C.; Mehmood, F.; Lam, T. L.; Chan, S. L.-F.; Wu, Y.; Yeung, C.-S.; Guan, X.; Li, K.; Chung, C. Y.-S.; Zhou, C.-Y.; Zou, T.; Che, C.-M. *Chem. Sci.* **2016**, *7*, 3123–3136. (c) Porras, J. A.; Mills, I. N.; Transue, W. J.; Bernhard, S. *J. Am. Chem. Soc.* **2016**, *138*, 9460–9472. (d) Reithmeier, R. O.; Meister, S.; Siebel, A.; Rieger, B. *Dalton Trans.* **2015**, *44*, 6466–6472. (e) Paul, A.; Das, N.; Halpin, Y.; Vos, J. G.; Pryce, M. T. *Dalton Trans.* **2015**, *44*, 10423–10430.
- (5) (a) Jiang, Y.; Li, G.; Che, W.; Liu, Y.; Xu, B.; Shan, G.; Zhu, D.; Su, Z.; Bryce, M. R. *Chem. Commun.* **2017**, *53*, 3022–3025. (b) Zhou, Y.; Xie, K.; Leng, R.; Kong, L.; Liu, C.; Zhang, Q.; Wang, X. *Dalton Trans.* **2017**, *46*, 355–363. (c) Zhao, Q.; Zhou, Y.; Li, Y.; Gu, W.; Zhang, Q.; Liu, J. *Anal. Chem.* **2016**, *88*, 1892–1899. (d) Song, Z.; Liu, R.; Li, Y.; Shi, H.; Hu, J.; Cai, X.; Zhu, H. *J. Mater. Chem. C* **2016**, *4*, 2553–2559. (e) Fan, Y.; Li, C.; Li, F.; Chen, D. *Biomaterials* **2016**, *85*, 30–39.
- (6) (a) Ma, D.-L.; Lin, S.; Wang, W.; Yang, C.; Leung, C.-H. *Chem. Sci.* **2017**, *8*, 878–889. (b) Jiang, B.; Gu, Y.; Qin, J.; Ning, X.; Gong, S.; Xie, G.; Yang, C. *J. Mater. Chem. C* **2016**, *4*, 3492–3498. (c) Zhang, K. Y.; Chen, X.; Sun, G.; Zhang, T.; Liu, S.; Zhao, Q.; Huang, W. *Adv. Mater.* **2016**, *28*, 7137–7142. (d) Ma, D.-L.; Chan, D. S.-H.; Leung, C.-H. *Acc. Chem. Res.* **2014**, *47*, 3614–3631.
- (7) (a) Nagai, Y.; Sasabe, H.; Takahashi, J.; Onuma, N.; Ito, T.; Ohisa, S.; Kido, J. *J. Mater. Chem. C* **2017**, *5*, 527–530. (b) Kim, M.-J.; Yoo, S.-J.; Hwang, J.; Park, S.-J.; Kang, J.-W.; Kim, Y.-H.; Kim, J.-J.; Kwon, S.-K. *J. Mater. Chem. C* **2017**, *5*, 3107–3111. (c) Lee, J.; Chen, H.-F.; Batagoda, T.; Coburn, C.; Djurovich, P. I.; Thompson, M. E.; Forrest, S. R. *Nat. Mater.* **2015**, *15*, 92–98. (d) Lo, K. K.-W. *Acc. Chem. Res.* **2015**, *48*, 2985–2995. (e) Lv, W.; Yang, T.; Yu, Q.; Zhao, Q.; Zhang, K. Y.; Liang, H.; Liu, S.; Li, F.; Huang, W. *Adv. Sci.* **2015**, *2*, 1500107. (f) Zhang, G.; Zhang, H.; Gao, Y.; Tao, R.; Xin, L.; Yi, J.; Li, F.; Liu, W.; Qiao, J. *Organometallics* **2014**, *33*, 61–68.
- (8) (a) Si, Y.; Qu, N.; Cui, L.; Gao, B.; Wu, Z. *Dalton Trans.* **2016**, *45*, 12587–12593. (b) Shang, X.; Han, D.; Zhang, H.; Zhou, L.; Zhang, G. *Eur. J. Inorg. Chem.* **2016**, *2016*, 1541–1547. (c) Ren, X.-Y.; Wu, Y.; Shan, G.-G.; Wang, L.; Geng, Y.; Su, Z.-M. *RSC Adv.* **2014**, *4*, 62197–62208.
- (9) (a) Ma, D.; Tsuboi, T.; Qiu, Y.; Duan, L. *Adv. Mater.* **2017**, *29*, 1603253. (b) Kim, J.-B.; Han, S.-H.; Yang, K.; Kwon, S.-K.; Kim, J.-J.; Kim, Y.-H. *Chem. Commun.* **2015**, *51*, 58–61. (c) Lee, S.; Kim, S.-O.; Shin, H.; Yun, H.-J.; Yang, K.; Kwon, S.-K.; Kim, J.-J.; Kim, Y.-H. *J. Am. Chem. Soc.* **2013**, *135*, 14321–14328. (d) Chi, Y.; Chou, P.-T. *Chem. Soc. Rev.* **2010**, *39*, 638–655.
- (10) (a) Gong, D.-P.; Gao, T.-B.; Cao, D.-K.; Ward, M. D. *Dalton Trans.* **2017**, *46*, 275–286. (b) Jiao, Y.; Li, M.; Wang, N.; Lu, T.; Zhou, L.; Huang, Y.; Lu, Z.; Luo, D.; Pu, X. *J. Mater. Chem. C* **2016**, *4*, 4269–4277. (c) Mills, I. N.; Kagalwala, H. N.; Bernhard, S. *Dalton Trans.* **2016**, *45*, 10411–10419. (d) Mei, Q.; Weng, J.; Xu, Z.; Tong, B.; Hua, Q.; Shi, Y.; Song, J.; Huang, W. *RSC Adv.* **2015**, *5*, 97841–97848. (e) Li, T.-Y.; Liang, X.; Zhou, L.; Wu, C.; Zhang, S.; Liu, X.; Lu, G.-Z.; Xue, L.-S.; Zheng, Y.-X.; Zuo, J.-L. *Inorg. Chem.* **2015**, *54*, 161–173. (f) Yang, X.; Zhou, G.; Wong, W.-Y. *Chem. Soc. Rev.* **2015**, *44*, 8484–8575.
- (11) (a) Steffen, A.; Costuas, K.; Boucekine, A.; Thibault, M.-H.; Beeby, A.; Batsanov, A. S.; Charaf-Eddin, A.; Jacquemin, D.; Halet, J.-F.; Marder, T. B. *Inorg. Chem.* **2014**, *53*, 7055–7069. (b) Lee, K. R.; Eum, M.-S.; Chin, C. S.; Lee, S. C.; Kim, I. J.; Kim, Y. S.; Kim, Y.; Kim, S.-J.; Hur, N. H. *Dalton Trans.* **2009**, 3650–3652.
- (12) (a) Wang, C.; Xiao, J. *Chem. Commun.* **2017**, *53*, 3399–3411. (b) Paneque, M.; Poveda, M. L.; Rendón, N. *Eur. J. Inorg. Chem.* **2011**, *2011*, 19–33. (c) Bleeke, J. R. *Acc. Chem. Res.* **2007**, *40*, 1035–1047.
- (13) Xu, H.; Huang, Z.-A.; Guo, X.; Yang, Y.; Hua, Y.; Cao, Z.; Li, S.; Xia, H. *Organometallics* **2015**, *34*, 4229–4237.
- (14) Frisch, M. J.; Trucks, G. W.; Schlegel, H. B.; Scuseria, G. E.; Robb, M. A.; Cheeseman, J. R.; Scalmani, G.; Barone, V.; Mennucci, B.; Petersson, G. A.; Nakatsuji, H.; Caricato, M.; Li, X.; Hratchian, H. P.; Izmaylov, A. F.; Bloino, J.; Zheng, G.; Sonnenberg, J. L.; Hada, M.; Ehara, M.; Toyota, K.; Fukuda, R.; Hasegawa, J.; Ishida, M.; Nakajima, T.; Honda, Y.; Kitao, O.; Nakai, H.; Vreven, T.; Montgomery, J. A., Jr.; Peralta, J. E.; Ogliaro, F.; Bearpark, M.; Heyd, J. J.; Brothers, E.; Kudin, K. N.; Staroverov, V. N.; Kobayashi, R.; Normand, J.; Raghavachari, K.; Rendell, A.; Burant, J. C.; Iyengar, S. S.; Tomasi, J.; Cossi, M.; Rega, N.; Millam, J. M.; Klene, M.; Knox, J. E.; Cross, J. B.; Bakken, V.; Adamo, C.; Jaramillo, J.; Gomperts, R.; Stratmann, R. E.; Yazyev, O.; Austin, A. J.; Cammi, R.; Pomelli, C.; Ochterski, J. W.; Martin, R. L.; Morokuma, K.; Zakrzewski, V. G.; Voth, G. A.; Salvador, P.; Dannenberg, J. J.; Dapprich, S.; Daniels, A. D.; Farkas, O.; Foresman, J. B.; Ortiz, J. V.; Cioslowski, J.; Fox, D. J. *Gaussian 09*, revision E.01; Gaussian, Inc.: Wallingford, CT, 2009.
- (15) Hay, P. J.; Wadt, W. R. *J. Chem. Phys.* **1985**, *82*, 299–310.
- (16) (a) Murase, T.; Yoshihara, T.; Tobita, S. *Chem. Lett.* **2012**, *41* (3), 262–263. (b) Murphy, M. P.; Smith, R. A. *J. Annu. Rev. Pharmacol. Toxicol.* **2007**, *47* (1), 629–656. (c) Murphy, M. P. *Trends Biotechnol.* **1997**, *15* (8), 326–330.
- (17) (a) Thorp-Greenwood, F. L. *Organometallics* **2012**, *31* (16), 5686–5692. (b) Li, S. P.-Y.; Liu, H.-W.; Zhang, K. Y.; Lo, K. K.-W. *Chem. - Eur. J.* **2010**, *16* (28), 8329–8339.
- (18) (a) Zaroni, K. P. S.; Coppo, R. L.; Amaral, R. C.; Murakami Iha, N. Y. *Dalton Trans.* **2015**, *44*, 14559–14573. (b) You, Y.; Park, S. Y. *Dalton Trans.* **2009**, 1267–1282. (c) Sajoto, T.; Djurovich, P. I.; Tamayo, A.; Yousufuddin, M.; Bau, R.; Thompson, M. E.; Holmes, R. J.; Forrest, S. R. *Inorg. Chem.* **2005**, *44*, 7992–8003.
- (19) (a) Xu, X.; Yang, X.; Wu, Y.; Zhou, G.; Wu, C.; Wong, W.-Y. *Chem. - Asian J.* **2015**, *10*, 252–262. (b) He, L.; Liao, S.-Y.; Tan, C.-P.; Lu, Y.-Y.; Xu, C.-X.; Ji, L.-N.; Mao, Z.-W. *Chem. Commun.* **2014**, *50*, 5611–5614. (c) Liu, Y.; Li, M.; Zhao, Q.; Wu, H.; Huang, K.; Li, F. *Inorg. Chem.* **2011**, *50*, 5969–5977.